

# The Water Vapor Sorption Behavior of Natural Fibers

Callum A. S. Hill,<sup>1</sup> Andrew Norton,<sup>2</sup> Gary Newman<sup>3</sup>

<sup>1</sup>Centre for Timber Engineering, School of Engineering and the Built Environment, Napier University, Edinburgh, United Kingdom

<sup>2</sup>Renueables Ltd, Llanillechid, Gwynedd, United Kingdom

<sup>3</sup>Plant Fibre Technology Ltd., Bangor, Gwynedd, United Kingdom

Received 7 September 2008; accepted 17 November 2008

DOI 10.1002/app.29725

Published online 5 February 2009 in Wiley InterScience (www.interscience.wiley.com).

**ABSTRACT:** The water vapor sorption behavior of a range of natural fibers (jute, flax, coir, cotton, hemp, Sitka spruce) has been studied. The data were analyzed using the Hailwood Horrobin model for isotherm fitting and determination of monolayer moisture content. The Hailwood Horrobin model was found to provide good fits to the experimental data. The extent of hysteresis exhibited between the adsorption and desorption isotherms was dependent on fiber type studied and was larger with high lig-

nin compared with low lignin content fibers. The area bounded by the hysteresis loop decreased as the isotherms were performed at progressively higher temperatures. This behavior is consistent with sorption interactions occurring with a glassy solid below the glass transition temperature. © 2009 Wiley Periodicals, Inc. *J Appl Polym Sci* 112: 1524–1537, 2009

**Key words:** adsorption; biofibers; hysteresis; swelling; water vapor

## INTRODUCTION

Apart from continued use in textile applications, interest in the study of the physical properties of natural fibers is increasing because of possible applications in composites. In part, this renewed interest is because of the generally lower embodied energy of natural fibers compared with glass fiber.<sup>1</sup> Natural fibers are also seeing increasing use as insulating materials, again mainly because of perceived superior environmental credentials compared with other products.<sup>2</sup> Another possible advantage of the use of natural fibers as insulation materials is their hygroscopicity. Used appropriately, they have the potential to act not simply as a passive insulation material, but they can also help to moderate extremes of humidity in an indoor environment. The use of natural fibers in such applications requires knowledge of their sorption behavior in the presence of atmospheric humidity under various conditions.

Plant-derived natural fibers (and wood) absorb atmospheric moisture due to the presence of hydroxyl (OH) groups associated with the cell wall macromolecules. These can be broadly classed into three types. Cellulose, which is the primary reinforcing element of the cell wall, is made of linear chains of glucose residues aggregated into microfibrillar units. These units possess a high crystalline content

(inaccessible to water molecules) but also a paracrystalline component to which water molecules can gain access. Thus, although the microfibril units have a high OH to C ratio, not all of the OH content is accessible. Lignin occurs in plant fibers in varying amounts, and is an amorphous crosslinked polymer composed of phenolic units and has a relatively low OH to C ratio compared with polysaccharides. The cell wall also contains a hemicellulose and pectic component, which is predominantly amorphous polysaccharide, is highly accessible to water molecules and has a high OH to C ratio. The cell wall of a plant fiber can thus be considered to be a natural composite material consisting of crystalline microfibrils embedded in an amorphous lignin/hemicellulose/pectic matrix. As the cell wall absorbs moisture, the sorbed water molecules occupy space between the microfibrils resulting in expansion of the material. The space that the water molecules occupy in the cell wall is referred to as the transient microcapillary network. Water within the cell wall is considered to be associated closely with the OH groups (monolayer water) or it occurs within the transient microcapillaries but is not intimately associated with the OH groups (polylayer water). Although cell wall bound water can be classified in this way, this is not to suggest that the situation is static because there is continual exchange of molecules between the monolayer and polylayer. However, it has been shown that the water molecules that are more closely associated with the OH groups are less mobile than those located in the polylayer.<sup>3</sup>

Correspondence to: C. A. S. Hill (c.hill@napier.ac.uk).

The water vapor sorption properties of natural fibers have been studied for many years because of their use in textile products, e.g.<sup>4-9</sup> The adsorption/desorption properties of cellulosic and lignocellulosic materials are characterized by the sigmoidal (IUPAC type II) shape of the isotherms and hysteresis between the sorption and desorption loops. If the sigmoidal adsorption line fit is extended to a projected value at 100% relative humidity (RH), this is often interpreted as being the so-called fiber saturation point (FSP) of the material. The FSP is a theoretical concept first defined by Tiemann<sup>10</sup> as being the moisture content (MC) of the sample when the cell wall is at saturation, but there is no water in the macrovoids (such as cell wall lumina) of the material. There are difficulties with this concept because the value found for FSP depends on the method used to determine it.<sup>11</sup> Methods where FSP is measured using samples where the cell wall is already water-saturated (such as solute exclusion), always give higher values for FSP than extrapolation of sorption isotherms.<sup>12</sup> Sorption isotherms cannot be accurately determined much above 95% RH in any case, and other methods, such as pressure plate, tension plate, or pressure membrane measurements, have to be used in this region.<sup>13</sup> The definition of FSP relies upon the assumption that there is a clean cut-off point where the cell wall is full of water and thereafter further sorption occurs within macrovoids such as lumens. It has shown experimentally that this does not occur in practice.<sup>14-16</sup> Nonetheless the literature on the subject contains many examples where this projection method of determining FSP is used.

The sigmoidal nature of the isotherms has been described by numerous models<sup>17-21</sup> and is considered to consist of three components. At low RH values (0-15%), monolayer adsorption onto the internal surface of the cell wall is the dominant process; between 15 and 70% RH, polylayer water formation in the transient cell wall microcapillaries occurs, and above 70% RH, capillary condensation becomes increasingly dominant. One model which continues to be used in the area of wood science to analyze the sigmoidal adsorption isotherm, but less so with natural fibers is the Hailwood Horrobin (HH) model.<sup>22</sup> This solid-solution model was developed to describe the sorption properties of cotton and has been extensively used to investigate the sorption behavior of wood or chemically modified wood.<sup>23-31</sup>

The Hailwood Horrobin (HH) model considers that water adsorbed by the cell wall can exist in two forms; called polylayer water and solid solution (monolayer water). Three chemical species that are therefore present in the cell wall are: unhydrated polymer, hydrated polymer, and polylayer water. These three components are assumed to behave as

an ideal solution. The H-H model examines the state of equilibrium existing between a vapor phase, a liquid phase, and a solid solution.

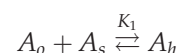
It is convenient to treat this in terms of molar concentrations. If  $X_o$  is assigned as the number of moles of unhydrated polymer,  $X_h$  is the number of moles of hydrated polymer (which is assumed to be equivalent to the number of moles of monolayer water), and  $X_s$  as the number of moles of polylayer water. The total number of moles of the three species is  $X_o + X_h + X_s$ . As it is assumed that this solution behaves as an ideal solution; the activities  $A_o$ ,  $A_h$ ,  $A_s$  of the three species are thus equal to their mole fractions in solution:

$$A_h = X_h / (X_o + X_h + X_s) \quad (1)$$

$$A_o = X_o / (X_o + X_h + X_s) \quad (2)$$

$$A_s = X_s / (X_o + X_h + X_s) \quad (3)$$

When an equilibrium condition exists between the three components, an equation of the form shown below can be written:



Hence:

$$K_1 = A_h / A_o A_s = X_h / X_o A_s \quad (4)$$

or

$$X_h = K_1 X_o A_s \quad (5)$$

There also exists an equilibrium state between the polylayer water and the water in the atmosphere given by its relative vapor pressure ( $p/p_o$ ) or  $h$ . The equilibrium constant for this system is given as:

$$K_2 = A_s / h \quad (6)$$

or

$$A_s = K_2 / h \quad (7)$$

The ratio  $X_h / (X_h + X_o)$  gives the moles  $X_h$  of hydrated polymer (and thus monolayer water) per mole of dry cell wall material. This is because the total number of moles of sites is equal to  $X_h + X_s$ . Combining eqs. (5) and (7) gives:

$$\frac{X_h}{X_h + X_o} = \frac{K_1 X_o K_2 h}{K_1 X_o K_2 h + X_o} = \frac{K_1 K_2 h}{K_1 K_2 h + 1} \quad (8)$$

The ratio  $X_s / (X_h + X_o)$  gives the moles of dissolved water per mole of dry cell wall polymer. This is obtained by rewriting eq. (3) in inverted form and

rearranging to give:

$$(X_h + X_o)/X_s = (1/A_s) - 1 = (1 - A_s)/A_s \quad (9)$$

Inverting, and using eq. (7) to eliminate  $A_s$ , gives:

$$\frac{X_s}{X_h + X_o} = \frac{K_2 h}{(1 - K_2 h)} \quad (10)$$

The sum of eqs. (8) and (10) gives the total number of moles of water in the cell wall per mole of dry plant material. This can be related to the cell wall moisture content  $M$ , because the moles of water are equal to the number of grams of water divided by the molecular weight of water (18), and that the moles of dry cell wall polymer are equal to the number of grams of dry cell wall material divided by the molecular weight of polymer per mole of sorption sites. As the latter is unknown, it will be represented by the symbol  $W$ . Thus,

$$\frac{X_h + X_s}{X_h + X_o} = \frac{W}{18} [(g \text{ hydrated water}) + (g \text{ dissolved water})] / (g \text{ dry polymer}) \quad (11)$$

$$\frac{X_h + X_s}{X_h + X_o} = (W/18)(m_h + m_s) = (W/18)m \quad (12)$$

where  $m_h$  and  $m_s$  are the fractional moisture contents of the monolayer and polylayer water, respectively, and  $m$  is the total fractional moisture content, all based on the dry weight of cell wall polymer. Equation 12 can be combined with eqs. (8) and (10) to give:

$$m = m_h + m_s = \frac{W}{18} \left( \frac{K_1 K_2 h}{1 + K_1 K_2 h} + \frac{K_2 h}{1 - K_2 h} \right) \quad (13)$$

or, in terms of relative humidity,  $H = 100h$ , and percentage moisture content  $M = 100m$ :

$$M = M_h + M_s = \frac{1800}{W} \left( \frac{K_1 K_2 H}{100 + K_1 K_2 H} \right) + \frac{1800}{W} \left( \frac{K_2 H}{100 - K_2 H} \right) \quad (14)$$

The classic sigmoidal shape of a sorption isotherm, is deconvoluted by the H-H model into a monomolecular ( $M_h$ ) and a polylayer ( $M_s$ ) component [eq. (14)].

Where  $M$  is the percentage moisture content at a given percentage relative humidity ( $H$ ),  $W$  is the molecular weight of cell wall polymer per sorption site and  $K_1$  and  $K_2$  are constants.

The values of  $K_1$  and  $K_2$  are determined by plotting  $H/M$  against  $H$ , which is predicted by H-H theory to give a parabolic relationship of the form shown in eq. (15).

$$\frac{H}{M} = A + BH - CH^2 \quad (15)$$

where  $K_1$ ,  $K_2$ ,  $W$ ,  $A$ ,  $B$ , and  $C$  are linked by the following relationships:

$$A = \frac{W}{18} \left[ \frac{1}{K_2(K_1 + 1)} \right] \quad (16)$$

$$B = \left( \frac{W}{18000} \right) \left[ \frac{K_1 - 1}{K_1 + 1} \right] \quad (17)$$

$$C = \left( \frac{W}{180000} \right) \left[ \frac{K_1 K_2}{K_1 + 1} \right] \quad (18)$$

From the above relationships, the values  $K_1$ ,  $K_2$ , and  $W$  can be derived as shown in eqs. (19)–(21).

$$K_1 = 1 + \frac{B^2 + B\sqrt{B^2 + 4AC}}{2AC} \quad (19)$$

$$K_2 = \frac{50(-B + \sqrt{B^2 + 4AC})}{A} \quad (20)$$

$$W = 1800\sqrt{B^2 + 4AC} \quad (21)$$

As with the BET theory, the isotherm in the HH model can be deconvoluted into a monolayer and polylayer component. However, though the monolayer in the BET model is invariant, that described in the HH model can change over the whole range of RH and is thus much more appropriate for an evolving surface associated with a material that changes in volume as adsorption proceeds. The HH model gives excellent agreement with experimental observations over a wide range of RH values although it does not explain hysteresis and is only suited to describing the adsorption part of the isotherm.

Hysteresis is widely encountered when the sorption properties of microporous materials are studied and there is a huge literature reporting hysteresis between the adsorption and desorption loops of water isotherms with natural fibers and wood. Various explanations can be advanced to explain the phenomenon. Adsorption of water into the material occurs when the substance is initially dry and leads to a stepwise filling of the cell wall microcapillaries by sorbed water layers whereas desorption occurs from the surface meniscus of water in these microcapillaries. However, the concept of a meniscus occurring in the cell wall microcapillaries (diameter of the order of 2–4 nm) is problematical.<sup>32</sup> Another explanation relies upon considering the geometry of the cell wall microcapillaries, where the throat of a

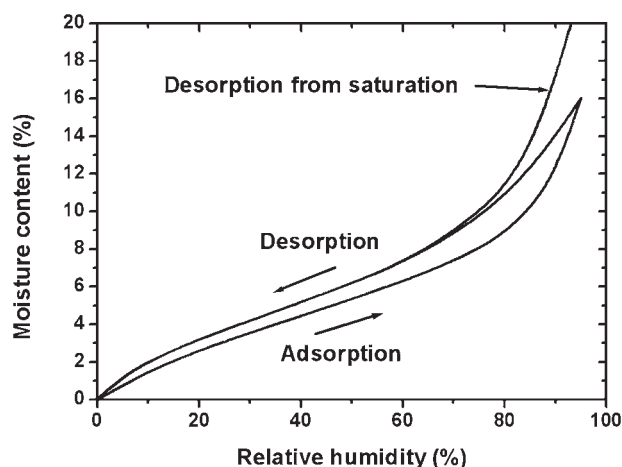


**Figure 1** Illustration of typical behavior exhibited by a lignocellulosic material when desorbing moisture from a fully water-saturated state and when desorbing moisture from a nonwater-saturated cell wall moisture content. Hysteresis between the adsorption and desorption isotherm is also shown.

microcapillary is of a smaller diameter than the interior (ink bottle).<sup>33</sup>

Chen and Wangaard<sup>34</sup> considered that differences between the adsorption and desorption loops were due to changes in contact angle between sorbed water and the internal surface of the wood material. In the desorption cycle, the water film in the internal microcapillaries of the cell wall is in contact with an already fully wet surface, whereas during adsorption the forming water film is in contact with a nonwetted surface. One problem with such an explanation is that when considering sorption processes involving the internal surface of the cell wall, concepts such as a liquid film or contact angle may not have any physical meaning. Chen and Wangaard noted this objection, but stated that their model would have application in the region where capillary condensation takes place. However, hysteresis occurs throughout the sorption range and not just in the capillary condensation region. The concept of surface wettability of water surfaces in microcapillaries has been used more recently in a theoretical treatment of sorption isotherms.<sup>35</sup> It should be noted in this context that two types of hysteresis can be observed with cellulose, or a lignocellulosic material (Fig. 1).

At any point on the adsorption cycle, the RH can be decreased again and the MC will also decrease, but will always exhibit a value greater than that observed during the adsorption cycle at a given RH. Furthermore, when the desorption isotherm is measured for a sample initially in a fully water-saturated state, the MC values thus obtained are higher than those found when the sample is desorbed from a MC below the FSP. This is known as an open hysteresis loop. It has been suggested that the higher MC

values obtained when desorbing from a saturated state are due to the microcapillaries collapsing accompanied by the formation of “permanent” hydrogen bonds which are no longer accessible on subsequent re-wetting cycles (hornification).<sup>11</sup> However, the same phenomenon is observed when a previously dry sample is re-wetted to saturation and subsequently desorbed.<sup>34</sup> Early work with cellulose suggested that hysteresis was an artifact caused by the presence of atmospheric gases within the sample and that if precautions were taken to remove these then it was no longer observed.<sup>36</sup> This work has only apparently been cited once, by Cohan in 1944.<sup>37</sup> However, a large number of experiments have been performed under carefully controlled vacuum conditions where hysteresis has still been observed. Stamm argues that the presence of such “permanent gases” in samples only affects hysteresis if the sample is nonswelling, rather than approximating to a gel system as is the case with cellulose or lignocellulosics.<sup>32</sup>

When the cell wall of a natural fiber absorbs moisture it swells, with the sorbed water molecules exerting pressure against restraining forces within the cell wall. As water is removed, the cell wall shrinks. This shrinkage is due not only to capillary forces acting within the of the cell wall, but the presence of lignin which also acts to collapse the microcapillaries.<sup>38</sup> This can be seen when cellulosic and lignocellulosic materials are dried using solvent exchange followed by supercritical CO<sub>2</sub>. Under such conditions, delignified material will exhibit surface areas in the excess of 100 m<sup>2</sup>g<sup>-1</sup>, whereas lignified material will only give values of 5 m<sup>2</sup>g<sup>-1</sup> or less. The difference is not simply because the lignin acts to occlude the cell wall microcapillaries, as a fully water-saturated lignified cell wall exhibits a much higher level of accessibility.<sup>38</sup>

Cassie<sup>39</sup> noted the importance of mechanical constraint acting upon sorbed water in wool fibers. In such cases, it was considered that the vapor pressure experienced by the absorbed water is influenced by the mechanical constraint exerted on the water as the fiber swells. It was stated that the isotherm could only be properly analyzed when this effect had been taken account of. When such an analysis was completed for an adsorption isotherm for wool, it was found that the characteristic sigmoidal shape was no longer observed. Similarly, the hysteresis effect in the isotherms was considered to be due to a mechanical effect only. This work does not appear to have been the subject of much further consideration in the literature. A serious problem with such an analysis is the reliance upon there being a meniscus in water present in pores of 5 nm and lower. It is well known that restraining wood from swelling reduces moisture adsorption, at least up until the



point where plastic flow of the wood occurs<sup>40</sup> no doubt a similar phenomenon would be observed in other lignocellulosic materials, although this has not been examined for plant fibers. As the cell wall of the plant fiber swells with increasing MC, new sorption sites are exposed. Thus the fiber presents an evolving surface under conditions of adsorption and desorption. Furthermore, there are differences in the accessibility of the material, because desorption is occurring from a swollen matrix with accessible OH groups associated with water molecules. By contrast, adsorption is associated with swelling of the matrix, thus exposing new OH sites.

It has been noted that in swelling gels the amount of hysteresis can be correlated with the elastic properties of the material.<sup>39</sup> The importance of matrix stiffness is also underlined by Lu and Pignatello<sup>41</sup> who note that the process of sorption in glassy solids results in the creation and expansion of microcapillaries and that this process is inelastic on the time scale of molecular diffusion. This inelasticity accounts for hysteresis as adsorption and desorption occur to and from different physical states of the solid. The glassy state is defined as a material having molecular-scale pores/capillaries embedded in a fluid-like matrix which is unable to fully relax to a thermodynamic equilibrium state due to the stiffness of the matrix macromolecules. Such a situation exists provided the sorption experiment is carried out at a temperature below the glass transition temperature of the matrix polymer. Similar explanations for hysteresis can be found in the earlier literature.<sup>42-44</sup>

Water adsorption into the plant cell wall is accompanied by a release of heat into the environment due to a reduction in energy of the water molecules as they are confined within the cell wall microcapillaries.<sup>17,45</sup> The heat energy released is in addition to the latent heat given off when water vapor condenses to a liquid. Measurement of this "heat of wetting" can use calorimetric methods (integral heat of wetting), or can be estimated by application of the Clausius-Clapeyron equation (differential heat of wetting).<sup>17,32</sup> As cellulose and lignocellulose exhibit sorption hysteresis, there have been objections to the use of the Clausius-Clapeyron equation because the materials cannot be in a true thermodynamic equilibrium with the environment.<sup>46</sup> To deal with this difficulty, Stamm and Loughborough<sup>47</sup> used what were termed "oscillating desorption" isotherm curves produced using large pieces of wood which established an intermediate isotherm between the adsorption and desorption loops. In Stamm and Loughborough's paper, the concept of hysteresis arising due to collapse of the microcapillary structure upon drying resulting in a reduced sorption capacity was invoked. While this is true when wood is dried from the green state, it does not apply to

the situation where the subsequently dried wood continues to display hysteresis on subsequent wetting and drying cycles. The data of Stamm and Loughborough were obtained at different temperatures and the thermodynamic properties calculated by application of the Clausius-Clapeyron equation. The validity of this approach can be questioned if it is considered that the wood is not in thermodynamic equilibrium with the environment under these circumstances. Although not explicitly stated, the data presented in Stamm and Loughborough's paper<sup>47</sup> appears to have been used in the United States Department of Agriculture Handbook No. 72 "Wood as an engineering material"<sup>48</sup> the data of which in turn has been used many times when various theoretical treatments of wood sorption are verified. Although the use of the Clausius-Clapeyron equation to determine differential heat of wetting may be questioned, there is undoubtedly an effect of temperature upon hysteresis, with the area enclosed by the hysteresis loop decreasing as the temperature at which the isotherm experiment is performed is raised.<sup>49,50</sup>

This study was undertaken to provide a comparative study of the sorption behavior of a range of natural fibers having application for use as insulation materials, as there are few studies in the literature where data for a wide range of fibers is given in one study. This study included fibers having both high and low lignin (flax, jute, coir, Sitka spruce, cotton, hemp) contents to determine what role (if any) lignin had to play in determining sorptive behavior and hysteresis effects. A further study was also undertaken on two fiber types (spruce and flax) to investigate the effect of temperature upon the sorptive properties and hysteresis. One original intention of this latter work was to determine the heat of wetting of flax fibers using the thermodynamic method described earlier. The results of this study are also presented and their validity discussed. This work was also extended to Sitka spruce as there is already a body of literature on the heat of wetting of spruce species. A dynamic vapor sorption (DVS) apparatus was used for this purpose, rather than the more usual use of saturated salt solutions. The DVS is able to provide highly accurate isotherms over a RH range that can be user set, and the temperature at which isotherms are recorded can be varied from 10 to 40°C.

## EXPERIMENTAL

Isotherm analyses were performed using a surface measurement system dynamic vapor sorption apparatus. This is a very useful means of determining accurate sorption isotherms at different temperatures and using a range of preset relative humidity values.

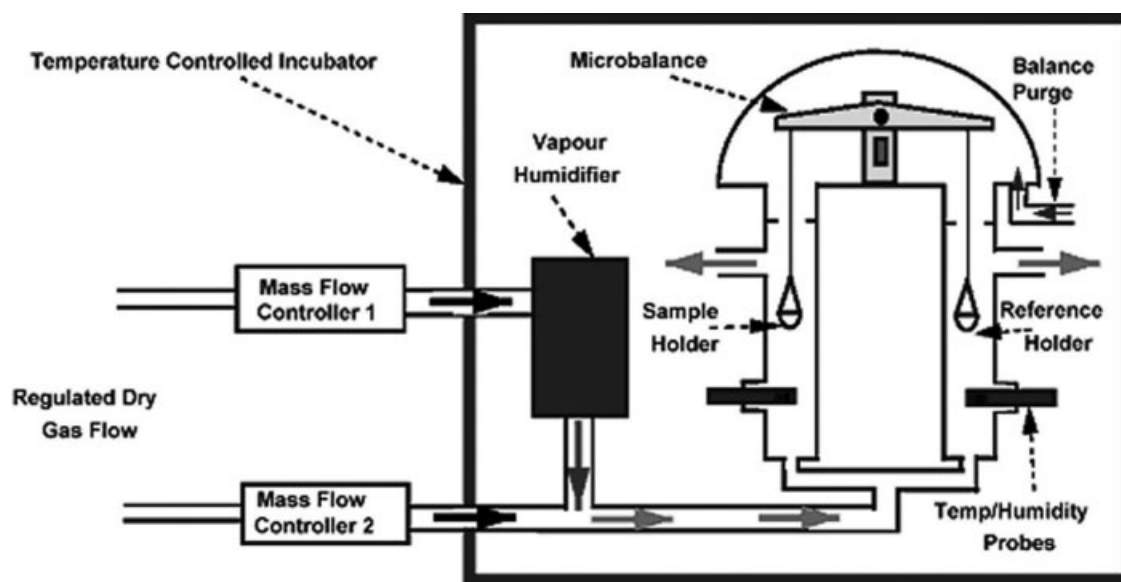


**Figure 2** Diagram showing the basic working principles of the surface measurement systems dynamic vapor sorption apparatus.

The apparatus contains two measurement pans (sample and reference holders) suspended from the arms of a Cahn ultra-sensitive microbalance, capable of measuring changes in sample mass as low as 1 part in 10 million (Fig. 2).

The sample and reference holders that are connected to the microbalance by hanging wires, sit in two arms of a chamber which is located in a thermostatically controlled cabinet. A constant flow of nitrogen gas into which nitrogen containing a preset amount of water vapor is mixed passes through the chamber to maintain a given RH. A typical run started at zero percent relative humidity and increased in 5% RH steps up to a maximum of 95% RH, before decreasing to zero percent RH in 5% RH steps. The instrument maintained a sample at a constant RH until the weight change per minute ( $dm/dt$ ) value reached 0.002% per minute, a value that from previous long-term exposure experiments yielded a sample MC within less than 0.1% of the equilibrium value at extended time.

Humidity and temperature probes are located in close proximity to the sample and reference holders providing direct measurement of these parameters. It was found that the temperature and humidity values were very stable during the tests. However, in practice both the RH and temperature were seldom exactly at the preset values and it was therefore necessary to use the actual RH and temperature values for each adsorption and desorption stage. The sample material was placed onto a pre-cleaned sample pan and carefully placed on the hang down wire connected to the microbalance, the sample chamber was closed and clamped. Once the sample pan was stationary the relative humidity was increased to

90% to discharge any static that had built up in the chamber or on the pan. Once the sample RH exceeded 90%, the RH was returned to a default value of 30% and a run commenced. Before a run commences, the instrument produces a “drying curve” with the RH set at zero percent until the sample weight is stable. An example run for an adsorption and desorption cycle is shown in Figure 3.

All natural fibers were used in an as-supplied state (supplied courtesy of the BioComposites Centre, Bangor, Gwynedd, UK), except for Sitka spruce which was ground down from small chips to fibers in a Wiley mill, no solvent extraction was employed prior to use. The following fiber types were studied: jute (*Corchorus capsularis*), coir (*Cocos nucifera*), flax (*Linum usitatissimum*), hemp (*Cannabis*

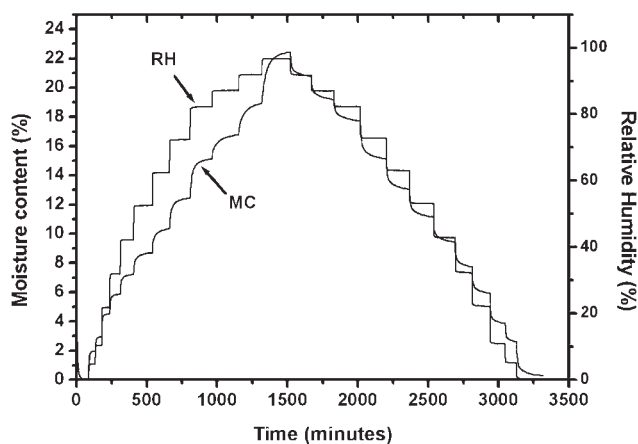


**Figure 3** Plot showing data from a typical DVS isotherm run for Sitka spruce at 25°C.

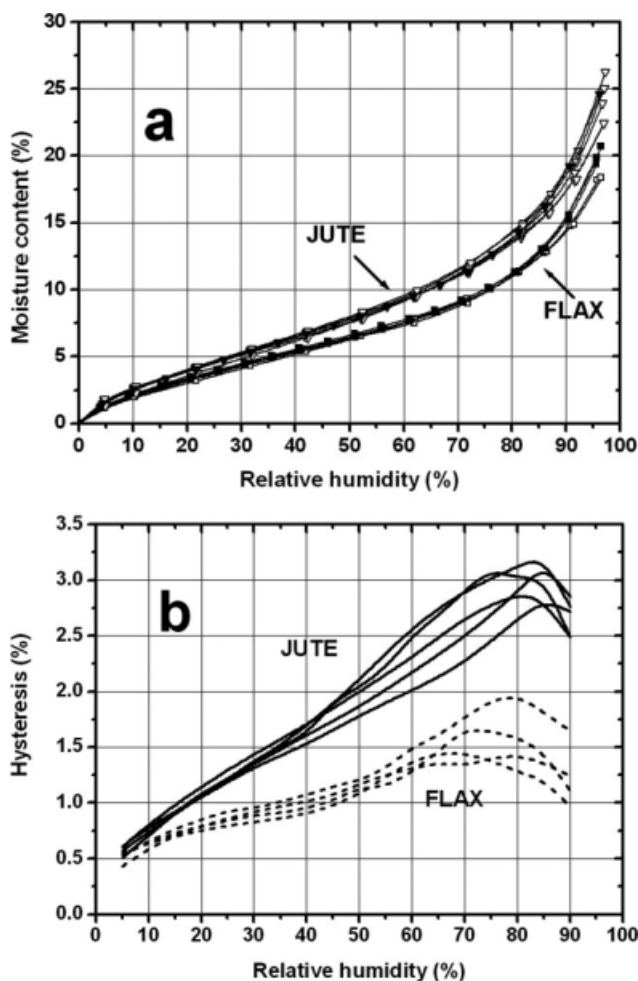


**Figure 4** Comparison of moisture adsorption behavior (a) and hysteresis of jute and flax (b). Filled symbols represent data measured at  $25.8 \pm 0.1^\circ\text{C}$  and open symbols data measured at  $24.5 \pm 0.1^\circ\text{C}$ .

*sativa*), cotton (*Gossypium barbadense*), Sitka spruce (*Picea sitchensis*).

## RESULTS AND DISCUSSION

### Reproducibility of data

Because the DVS apparatus used for this study was only able to measure one sample at a time, some preliminary studies were undertaken to determine the reproducibility of the sorption process using samples of jute and flax, the results of which are shown in Figure 4. These sorption curves [Fig. 4(a)] show that the data for different samples of the same fiber type were reproducible over most of the RH range studied but that deviation in the data occurred above  $\sim 70\%$  RH. With flax, the differences were apparently related to a slight difference in the temperature of the experiment ( $1^\circ\text{C}$ ), but no such relationship was observed with coir, where the variation was random. Differences were also found in the

extent of hysteresis between the sorption and desorption cycles, although there were clear differences in behavior between the flax and jute fibers [Fig. 4(b)]. From this it was concluded that differences in sorption and desorption isotherms of different fiber types could be reliably determined below 70% RH, and differences were discernable up to 90% RH, but that some caution had to be exercised when determining differences in hysteresis with different fibers due to the scatter observed. The wider range of MCs found above 70% RH corresponds to the region where capillary condensation becomes increasingly dominant and this might not be a fiber-specific property. In addition, quite apart from the problems associated with determining the FSP by projecting the adsorption isotherms to 100% RH noted in the introduction, the level of scatter of data above 70% RH leads to a considerable variation in the determined FSP value (greater than 5% MC) in any case.

### Comparison of different fibers

Individual moisture adsorption/desorption isotherms are shown in Figure 5 for the following fibers: jute [Fig. 5(a)], coir [Fig. 5(b)], flax [Fig. 5(c)], Sitka spruce [Fig. 5(d)], hemp [Fig. 5(e)], cotton [Fig. 5(f)]. All of the fiber types studied exhibited the classic Type II sigmoidal adsorption and desorption isotherms, although there were considerable differences in the total amount of moisture present in the samples at a given RH, as well as the degree of hysteresis exhibited.

The differences in adsorption and desorption behavior are more clearly illustrated when the curves are overlaid as shown in Figure 6(a) (adsorption) and Figure 6(b) (desorption). Jute, coir and Sitka spruce exhibited higher MCs on adsorption and desorption compared with fibers having very low lignin levels (hemp, flax, cotton), although hemp exhibited higher MCs in the capillary condensation region. Cotton had the lowest level of moisture uptake of all the fibers studied. Many factors influence the moisture sorption properties of natural fibers, of which OH accessibility is a significant component. Cotton has a high level of crystalline cellulose, low levels of amorphous polysaccharide and no phenolic content; accessible OH content is low compared to the other fibers studied, explaining the low moisture uptake.

The reason more highly lignified fibers showed higher MCs may be related to the ability of the lignin network to deform to accommodate water within the cell wall. The OH to unit mass ratio is lower than with polysaccharide materials, thus OH accessibility would be lower in lignified compared with polysaccharide-rich materials (this could be verified using deuterium exchange experiments<sup>51,52</sup>).

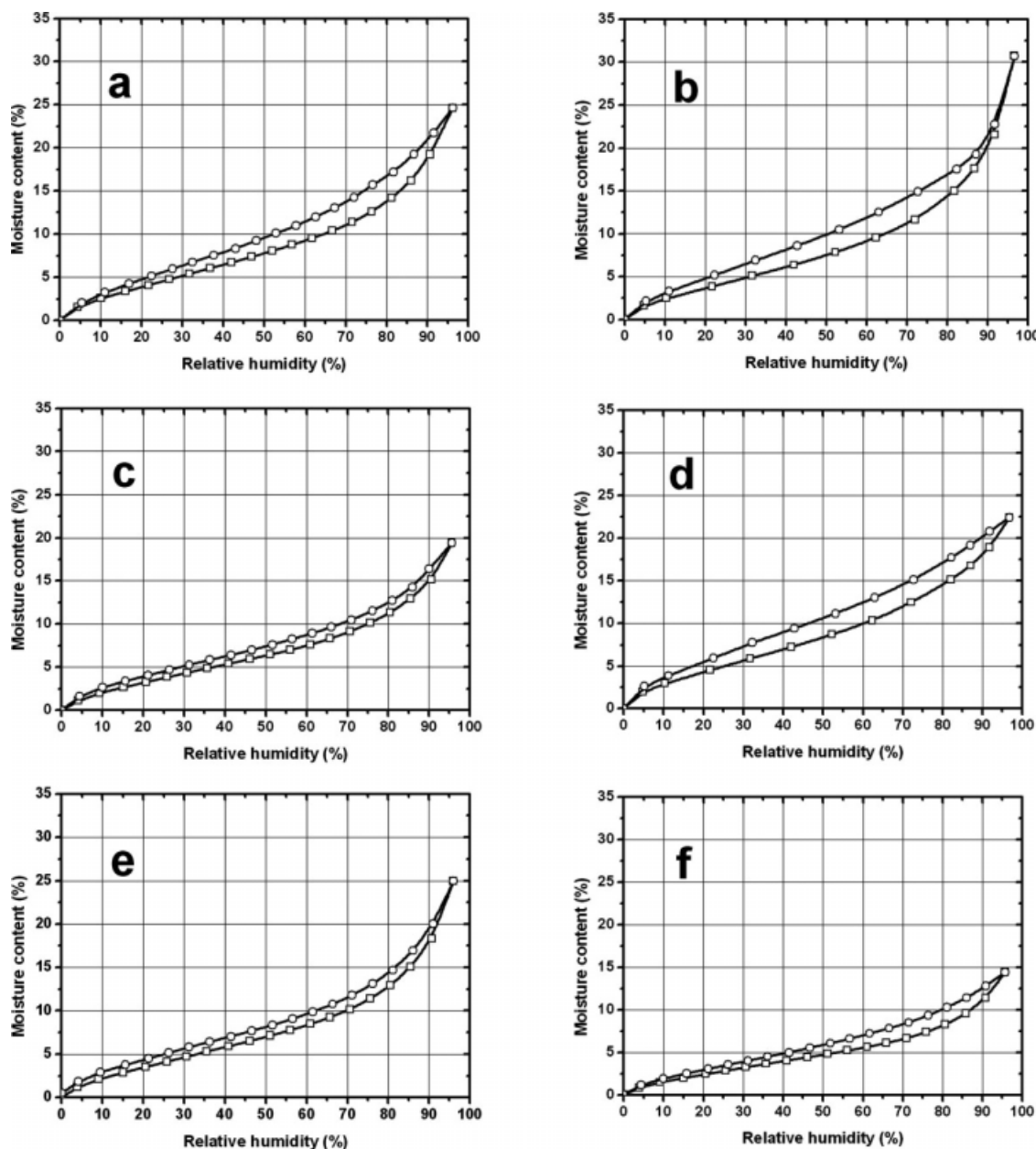


**Figure 5** Moisture adsorption and desorption behavior for jute (a), coir (b), flax (c), Sitka spruce (d), hemp (e), cotton (f), at 25°C.

The lignin-rich fibers were also found to have larger hysteresis loops compared with the polysaccharide-rich fibers (Fig. 7). This behavior is consistent with the explanation for hysteresis given by Lu and Pignatello.<sup>41</sup> Sorbent deformation in the presence of sorbates has been suggested as the universal cause of sorptive hysteresis in swelling substrates.<sup>53</sup> During sorption, microcapillaries in the cell wall are caused to expand due to the thermal motion of the incoming water molecules thus creating new internal surface. During desorption, relaxation of the matrix to the state it was in during adsorption is kinetically hindered.<sup>54</sup> The free volume (that is internal cell wall space not occupied by macromolecules; also termed microcapillaries) is greater on desorption

compared to adsorption, hence adsorption and desorption are occurring within different physical environments.<sup>55</sup> The effect of matrix crosslinking upon hysteresis was tested using humic soils treated with  $\text{Al}^{3+}$  ions, where it was found that increased hysteresis was linked to a higher crosslinking density.<sup>56</sup> Although the polysaccharide-rich fibers exhibited less hysteresis, there is an indication that although cotton showed the lowest level of hysteresis below 50% RH, above this RH level, hysteresis exhibited by cotton was apparently greater than with flax or hemp. This effect (if real) may be related to the amorphous polysaccharide content providing a greater degree of cell wall deformation relaxation with flax and hemp compared with cotton.



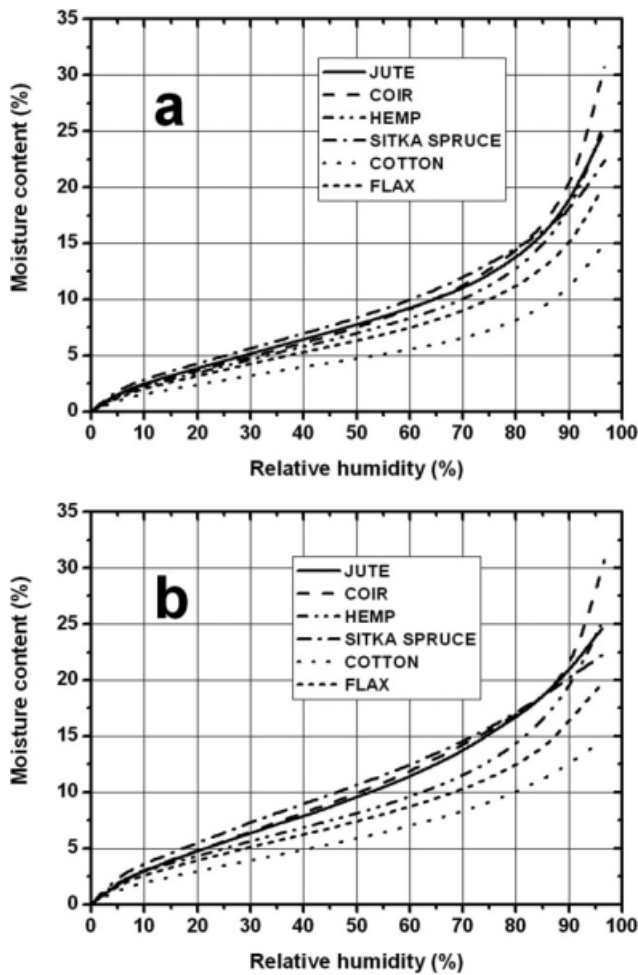


**Figure 6** Graph comparing the moisture adsorption (a) and desorption (b) behavior of the six natural fibers investigated in this study.

To further understand the effect of the amorphous polysaccharide content upon sorption behavior, flax was compared with Duralin (Fig. 8). Duralin is a fiber that was produced from flax by Ceres BV of the Netherlands using a hydrothermal treatment process which is closely related to the commercial Platowood process<sup>13</sup> although Duralin production has now ceased. This process degrades the amorphous polysaccharide components of the cell wall, and increases the proportion of crystalline polysaccharide content. In addition, breakdown compounds of the hemicelluloses form furfuryl which may participate in cross-linking reactions.<sup>57</sup> The Duralin exhibited lower levels of sorption compared with flax in agreement with previous reports on this material.<sup>57–59</sup>

The hysteresis of the Duralin was less than that exhibited by flax below 70% RH, but exceeded that of flax above this RH. The reason for this change could be related to matrix stiffness being increased by crosslinking and loss of amorphous polysaccharide material, but then an increase in hysteresis would be expected throughout the RH range.

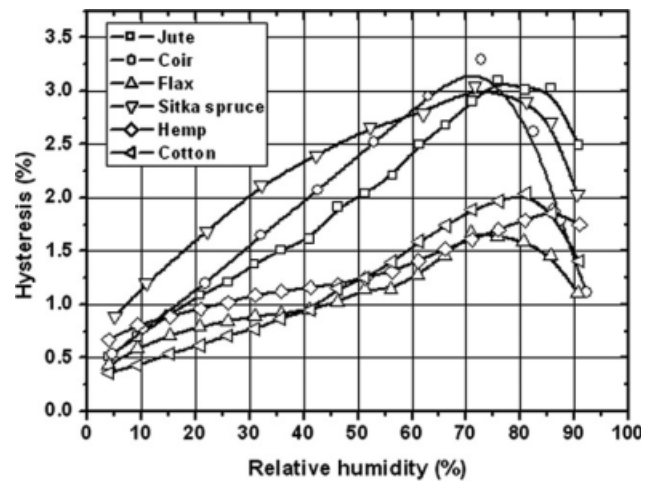


**Figure 7** Hysteresis between adsorption and desorption curves (obtained by subtraction of equilibrium moisture contents) for various natural fibers at different values of relative humidity.

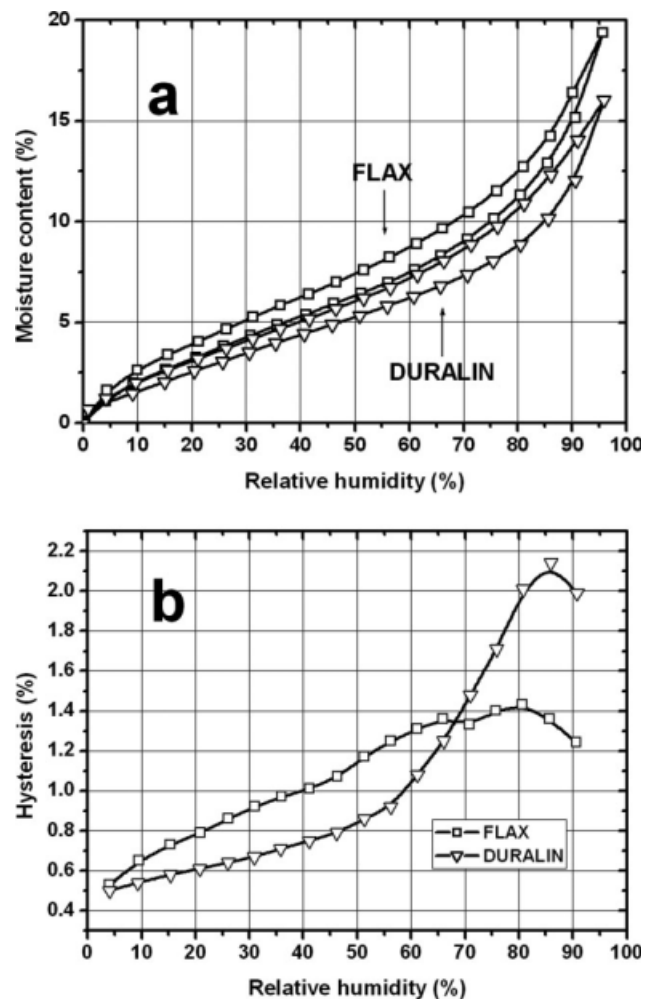


**Figure 8** Comparison of adsorption and desorption behavior of flax and Duralin<sup>TM</sup>.

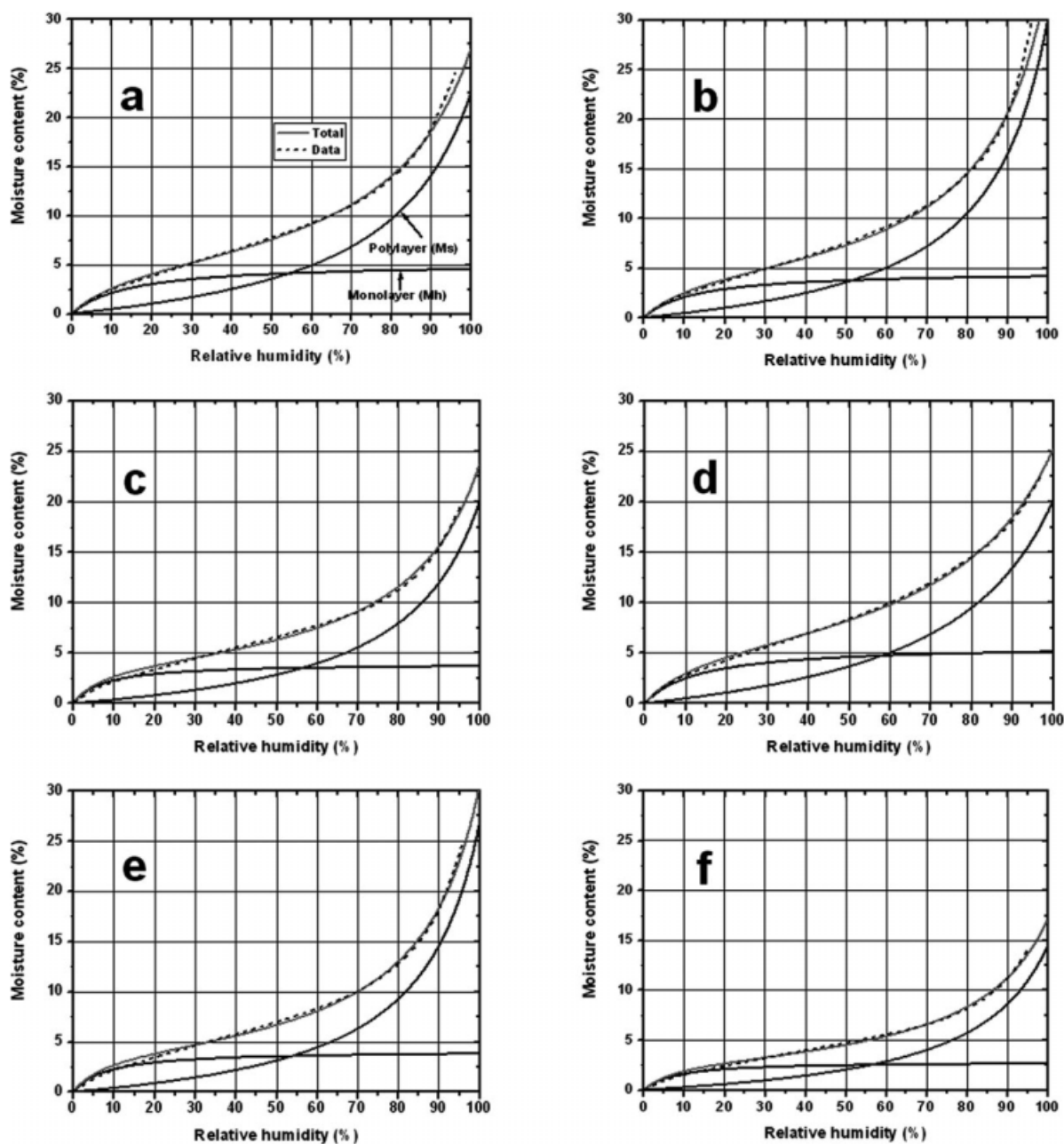


**Figure 9** Comparison of monolayer, polylayer calculated using the Hailwood Horrobin model, and sum of polylayer and monolayer (total) adsorption isotherm fits with a best fit line through the adsorption isotherm data. For the following natural fibers jute (a), coir (b), flax (c), Sitka spruce (d), hemp (e), cotton (f).

Another possible explanation is related to the formation of voids and fissures in the cell wall due to the hydrothermal treatment, resulting in capillary effects being dominant at the higher RH range with Duralin.

#### Hailwood Horrobin fitting to the data

The results from the HH fits to the data for the six fibers are presented in Figure 9. These deconvolute the sigmoidal isotherms into monolayer ( $M_h$ ) and polylayer ( $M_s$ ) water. The fits are generally satisfac-

tory although in the case of jute [Fig. 9(a)] and coir [Fig. 9(b)] the total MC above 90% RH ( $M_h + M_s$ ) is slightly overestimated; while for flax [Fig. 9(c)], hemp [Fig. 9(e)] and cotton [Fig. 9(f)] the total MC in the region 10–20% RH is slightly overestimated.

From the fitting parameters (Table I), values for  $M_h$ ,  $M_s$  and total water ( $M_h + M_s$ , giving a crude estimate of “FSP”) at 100% RH are given in Table II. If it is assumed that  $M_h$  is related to the number of primary sorption sites (OH groups) in the cell wall, then these data can be used to determine the number of accessible OH groups in each of the fiber

**TABLE I**  
Values for Monolayer ( $M_h$ ) and Polylayer ( $M_s$ ) Water Derived from Hailwood Horrobin fits Projected to 100% Relative Humidity

Fiber	$M_h$ (%)	$M_s$ (%)	$M_h + M_s$ (%)
Jute	4.53	22.44	26.97
Coir	4.14	29.84	33.98
Flax	3.68	19.92	25.60
Sitka spruce	5.10	20.08	25.18
Hemp	3.79	26.65	30.44
Cotton	2.65	14.38	17.03

species studied. It is also possible to estimate the number of OH groups from the polymeric cell wall composition of the fibers using the data given in Table III, using the method described in detail by Rowell.<sup>60</sup> It can be seen (Table IV) that the calculated OH content and that determined from the monolayer water content do not correspond, even when some account is taken of there being inaccessible OH content associated with the crystalline cellulose (assumed at 60% for all fibers). Although this is a very crude estimate of OH content, it nonetheless demonstrates that there is problem with assuming that OH content can be determined from the monolayer water content and this has been remarked upon previously with work on Corsican pine.<sup>27</sup> As noted earlier, a determination of accessible OH content requires the use of deuterium exchange or other appropriate experimental techniques.

#### Effect of temperature on isotherms and heat of wetting

The sorption behavior of flax and Sitka spruce at different temperatures is shown in Figure 10. Increasing the temperature did not affect the adsorption isotherm of flax, but did result in a slight drift to the right with the adsorption isotherm of Sitka spruce (resulting in a slightly lower MC at a given RH). However, the desorption isotherm did show significant changes with both species with the isotherm moving to the right as temperature increased. The hysteresis loops exhibited the two species decreased significantly as the isotherm temperature was increased, which again, is behavior consistent with

**TABLE II**  
Hailwood Horrobin Fitting Parameters

Fiber	A	B	C	$K_1$	$K_2$	W
Jute	2.506	0.152	0.00140	8.47	0.812	346.9
Coir	2.449	0.172	0.00167	9.12	0.865	385.7
Flax	1.744	0.224	0.00199	16.39	0.834	455.5
Sitka spruce	2.067	0.141	0.00122	9.76	0.777	311.7
Hemp	1.823	0.213	0.00198	14.46	0.867	439.6
Cotton	2.479	0.310	0.00276	15.98	0.835	632.4

**TABLE III**  
Approximate Polymeric Composition (wt %) of the Cell Wall of Plant Fibers Studied

Fiber	Cellulose (%)	Hemicellulose/pectin (%)	Lignin (%)	Ref.
Jute	72	14	13	63
Coir	43	5	45	63
Flax	81	16	3	63
Sitka spruce	45	25	30	64
Hemp	74	19	4	63
Cotton	94	6	0	63

the description of hysteresis in a glassy solid. As the isotherm temperature is increased, the size of the hysteresis loop is predicted to decrease until the glass transition temperature of the material is reached, at which point it becomes zero. The glass transition temperature of lignin in the presence of moisture is in the region of 60 to 90°C<sup>61</sup> and linear projections of the decrease in hysteresis loops reached zero in this temperature range for Sitka spruce.

With flax, linear projections of the decrease in hysteresis to zero fell within the temperature range of 65 to 85°C, but no information on the possible glass transition temperature of cell wall matrix material has been located for flax. The near disappearance of the hysteresis loop at around 100°C has been commented upon in the literature previously.<sup>42</sup> As noted in the introduction, the Clausius-Clapeyron equation has been used to determine the heat of wetting of wood and other natural materials, such as fibers and foodstuffs. However, the use of such a thermodynamic method requires that the material is in equilibrium with its environment (the chemical potential of water molecules in the vapor and the cell wall are equal), but the phenomenon of hysteresis indicates

**TABLE IV**  
Estimation of OH Concentration (in mmoles per gram) of Dry Cell Wall Substance from Monolayer Water Content at 100% RH Obtained from the Hailwood-Horrobin Fits

Fiber	HH monolayer OH concentration	Totally accessible calculated OH concentration	OH concentration (60% crystalline cellulose)
Jute	2.5	16.5	8.5
Coir	2.3	11.7	6.6
Flax	2.0	17.9	8.8
Sitka spruce	2.8	14.2	9.2
Hemp	2.1	17.7	9.2
Cotton	1.5	18.4	8.0

Data is compared with approximate OH concentration for totally accessible OH content and for concentration based on 60% crystalline (and hence inaccessible) cellulose OH content.

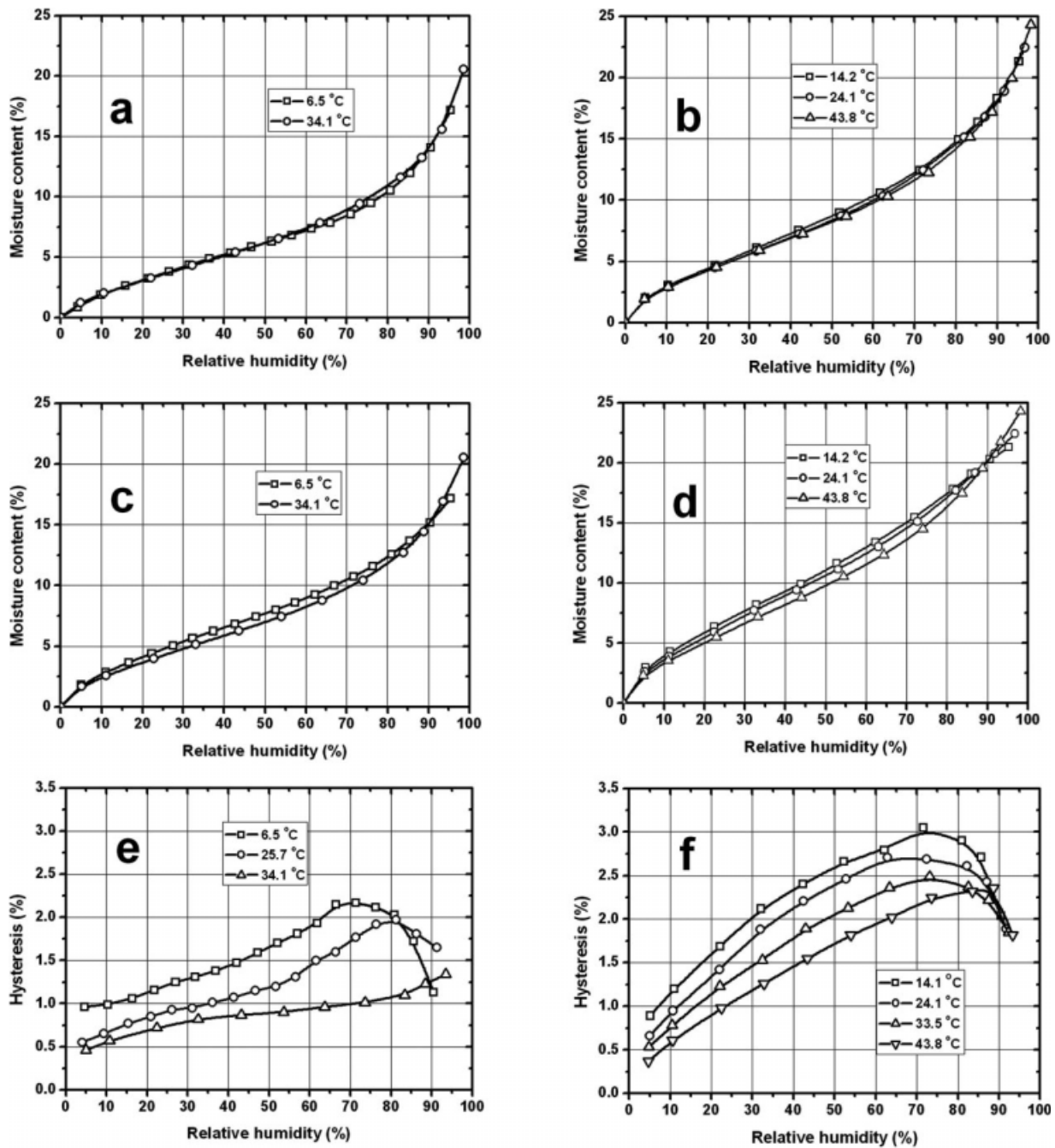
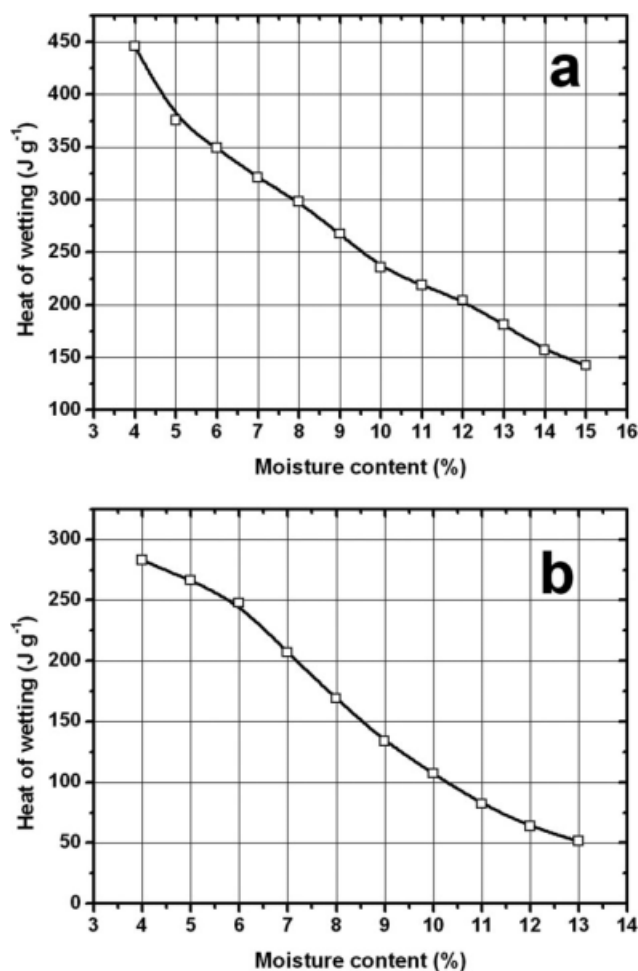


Figure 10 Effect of isotherm temperature on adsorption, desorption, and hysteresis for flax (a, c, e, respectively) and Sitka spruce (b, d, f, respectively).

that this state of thermodynamic equilibrium does not apply. For this reason, Stamm employed the method of “swinging isotherms,” which give the same line on adsorption or desorption. However, if hysteresis is attributable to the swelling property of the material, then both the adsorption and desorption cycles represent a state of local equilibrium of the material with the environment, with the chemical potential of the water in the cell wall being dependent upon the previous sorption history. Thus

the method to determine heat of wetting from the adsorption or desorption isotherm using the Clausius-Clapeyron equation should be valid. However, the use of the “swinging isotherm” is not valid because this does not represent a state of thermodynamic equilibrium of the material with its surroundings. In this study, little or no change was found in the adsorption isotherm with different temperatures, thus the desorption isotherm data were used and the Clausius-Clapeyron equation applied.<sup>18</sup>





**Figure 11** Heat of wetting as determined from the desorption isotherms at different temperatures using the Clausius-Clapeyron equation for Sitka spruce (a) and flax (b).

$$Qv = -1.06172 \times (\log p_1 - \log p_2) / (1/T_1) - (1/T_2) \quad (22)$$

where  $Qv$  is the heat of wetting,  $p_1$  is the partial vapor pressure of water vapor at absolute temperature  $T_1$  and  $p_2$  is the partial vapor pressure of water vapor at absolute temperature  $T_2$ .

The data for Sitka spruce are presented in Figure 11, where the heat of wetting shows an apparently linear decrease with cell wall MC. The values obtained in this study were compared with the literature<sup>62</sup> where it was found that reasonable agreement was obtained with the literature in the MC range 10–15%, but that the literature values are higher at lower moisture contents. The MC range used for analysis in this study was narrower than that given in the literature because it was considered that data were not reliable outside the range studied herein. In the low MC range, the isotherms approach one another and begin to curve down to 0% MC and

the lack of data points over the 0–5% MC range makes the projected lines unreliable in this region. At MCs much above 16% the desorption isotherm lines again begin to approach one another and actually cross one another at 20% MC (spruce) and 15% MC (flax), also making this region of the data unreliable.

The total area under the line running from 0% MC to cell wall saturation is the integral heat of wetting, the value of which is related to the total sorptive capacity of the cell wall, but not the total number of primary sorption sites. The differential heat of wetting at 0% MC is related to the type of sorption site that interacts with the water molecule. Unfortunately, the data obtained from this study did not allow for sufficiently robust evaluations of these two parameters.

## CONCLUSIONS

This study has shown that there are considerable differences in the adsorption/desorption behavior between different natural fibers. The area bounded by the hysteresis loop between the adsorption and desorption isotherms was found to be large for high lignin content compared with low lignin content or lignin-free fibers. Increasing the temperature at which the isotherm was determined caused the desorption isotherm to shift to the right resulting in a smaller hysteresis loop. This behavior is consistent with sorption interactions with glassy solids below the glass transition temperature. The material exhibits quasi-static equilibria under conditions of sorption and desorption, but transition between these two states is kinetically hindered. However, the material is in equilibrium with the environment under both adsorption and desorption, and it is therefore legitimate to use thermodynamic analyses of the processes. Analysis of the adsorption isotherms using the Hailwood Horrobin model gave satisfactory fits to the data. However, equating the magnitude of the monolayer with the primary sorption sites is not appropriate.

## References

- Baillie, C., Ed. *Green Composites—Polymer Composites and the Environment*; CRC Press: Boca Raton, FL, 2004.
- Collet, F.; Bart, M.; Serres, L.; Miriel, J. *Constr Build Mat* 2008, 22, 1271.
- Walker, J. C. F. *Primary Wood Processing—Principles and Practice*; Springer: The Netherlands, 2006, Chapter 3.
- Assaf, A. G.; Haas, R. H.; Purves, C. B. *J Am Chem Soc* 1944, 66, 66.
- Chakravarty, A. C. *Text Res J* 1958, 28, 878.
- Chatterjee, H. *Text Res J* 1962, 32, 694.
- Cookson, P. G.; Slota, I. J. *Text Res J* 1993, 63, 495.
- Mizutani, C.; Tsujii, Y.; Bertoniere, N. *Text Res J* 1999, 69, 559.

9. Bessadok, A.; Marais, S.; Roudesli, S.; Lixon, C.; Métayer, M. *Compos A* 2008, 39A, 29.
10. Tiemann, D. USDA Forest Service Bulletin Number 70, 1906.
11. Stamm, A. J. *Wood Sci* 1971, 4, 114.
12. Hill, C. A. S. *Holzforschung* 2008, 62, 423.
13. Hill, C. A. S. *Wood Modification: Chemical, Thermal and Other Processes*; Wiley: Chichester, UK, 2007.
14. Almeida, G.; Hernández, R. E. *Wood Sci Technol* 2006, 40, 599.
15. Almeida, G.; Hernández, R. E. *Wood Fiber Sci* 2006, 36, 74.
16. Hernández, R. E.; Pontin, M. *Wood Fiber Sci* 2006, 38, 474.
17. Siau, J. F. *Transport Processes in Wood*; Springer-Verlag: Berlin, 1984.
18. Skaar, C. *Water in Wood*; Syracuse University Press: New York, 1972.
19. Simpson, W. *Wood Fiber Sci* 1980, 12, 183.
20. Venkateswaran, A. *Chem Rev* 1970, 70, 619.
21. Okoh K. I. A.; Skaar, C. *Wood Fiber Sci* 1980, 12, 98.
22. Hailwood, A. J.; Horrobin, S. *Trans Faraday Soc* 1946, 42B, 84.
23. Spalt, H. A. *Forest Prod J* 1958, 8, 288.
24. Popper, R.; Bariska, M. *Holz Roh Werkst* 1972, 30, 289.
25. Yasuda, R.; Minato, K.; Norimoto, M. *Holzforschung* 1995, 49, 549.
26. Chen, Z.; Lamb, F. M. *Wood Fiber Sci* 2002, 34, 553.
27. Papadopoulos, A. N.; Hill, C. A. S. *Wood Sci Technol* 2003, 37, 221.
28. Nzokou, P.; Kamden, D. P. *Wood Fiber Sci* 2004, 36, 483.
29. Papadopoulos, A. N.; Avramidis, S.; Elustondo, D. *Wood Sci Technol* 2005, 39, 99.
30. Popper R.; Niemz, P.; Torres, M. *Holz Roh Werkst* 2006, 64, 491.
31. Hamdan, H.; Hill, C. A. S.; Zaidon, A.; Anwar, U. M. K.; Abd. Latif, M. *J Trop For Sci* 2007, 19, 18.
32. Stamm, A. J. *Wood and Cellulosic Chemistry*; Ronald Press: New York, USA, 1964.
33. Koch, P. *Utilization of the Southern Pines*, U.S. Department of Agriculture Forest Service, Vol.1, 1972, p 279.
34. Chen, C-M.; Wangaard, F. F. *Wood Sci Technol* 1968, 2, 177.
35. Churaev, N. V.; Setzer, M. J.; Adolphs, J. *J Colloid Interface Sci* 1998, 197, 327.
36. Hamm, H. A.; Patrick, W. A. *Text Res J* 1936, 6, 401.
37. Cohan, L. H. *J Am Chem Soc* 1944, 66, 98.
38. Papadopoulos A. N.; Hill, C. A. S. *J I. Wood Sci* 2001, 15, 337.
39. Cassie, A. B. D. *Trans Faraday Soc* 1945, 41, 458.
40. Tarkow, H. In *Wood: Its Structure and Properties*; Wangaard, F. F., Ed.; Pennsylvania State University: Pennsylvania, 1980.
41. Lu, Y. L.; Pignatello, J. J. *Env Sci Technol* 2004, 38, 5853.
42. White, H. J.; Eyring, H. *Text Res J* 1947, 17, 523.
43. Urquhart, A. R.; Eckersall, N. *J Text Inst* 1929 20, T125.
44. Barkas, W. W. *Trans Faraday Soc* 1942, 38, 194.
45. Morrison, J. L.; Dzieciuch, M. A. *Can J Chem* 1959, 37, 1379.
46. Ehrlich, S. H.; Bettelheim, F. A. *J Phys Chem* 1963, 67, 1954.
47. Stamm, A. J.; Loughborough, W. K. *J Phys Chem* 1934, 39, 121.
48. U.S. Department of Agriculture. *Wood Handbook: Wood as an Engineering Material*. United States Department of Agriculture Forest Service Handbook No. 72, Revised 1974.
49. White, H. J.; Eyring, H. *Text Res J* 1947, 17, 523.
50. Gupta, S. L.; Bhatia, R. K. S. *Text Res J* 1971, 41, 97.
51. Taniguchi, T.; Harada, H.; Nakato, K. *Nature* 1978, 272, 230.
52. Phuong, L. X.; Tkayama, M.; Shida, S.; Matsumoto, Y.; Aoyagi, T. *Holzforschung* 2007, 61, 488.
53. Tvardovski, A. V.; Fomkin, A. A.; Tarasevich, Y. I.; Zhukova, A. I. *J Colloid Interface Sci* 1997, 191, 117.
54. Lu, Y.; Pignatello, J. J. *Environ Sci Technol* 2002, 36, 4553.
55. Sander, M.; Lu, Y.; Pignatello, J. J. *J Environ Qual* 2005, 34, 1063.
56. Lu, Y.; Pignatello, J. J. *J Environ Qual* 2004, 33, 1314.
57. Pott, G. T. In *Natural Fibers Plastics and Composites*; Wallenberger, F. T.; Weston, N., Eds.; Kluwer: Dordrecht, The Netherlands, 2004, Chapter 8.
58. Stamboulis, A.; Baillie, C. A.; Peijs, T. *Compos A* 2001, 32, 1105.
59. Bismark, A.; Aranberri-Askargorta, I.; Pringer, J.; Lampke, T.; Wielage, B.; Stamboulis, A.; Shenderovich, I.; Limbach, H. H. *Polym Compos* 2002, 23, 872.
60. Rowell, R. M. *Wood Sci* 1980, 13, 102.
61. Xia, G.; Pignatello, J. J. *Environ Sci Technol* 2001, 35, 84.
62. Rowell, R. M., Ed. *The Chemistry of Solid Wood—American Chemical Society Advances in Chemistry Series, No. 207*; American Chemical Society: Washington DC, 1984.
63. Bolton, A. J. *Mater Tech* 1994, 9, 12.
64. Fengel, D.; Wegener, G. *Wood—Chemistry Ultrastructure Reactions*; Walter de Gruyter: Berlin, Germany, 1984.